Available online at www.sciencedirect.com
ScienceDirect
Applied Acoustics 68 (2007) 739–751
applied acoustics
www.elsevier.com/locate/apacoust

Vibro-acoustic analysis of a rectangular-like cavity with a tilted wall

Y.Y. Li [1], L. Cheng *

Department of Mechanical Engineering, The Hong Kong Polytechnic University, Hung Hom, Kowloon, Hong Kong SAR, China

Received 30 March 2006; received in revised form 6 April 2006; accepted 11 April 2006
Available online 12 June 2006

Abstract

In this paper, a fully coupled vibro-acoustic model is developed to characterize the structural and acoustic coupling of a flexible panel backed by a rectangular-like cavity with a slight geometrical distortion, which is introduced through a tilted wall. The combined integro-modal approach is used to handle the acoustic pressure inside the irregular-shaped cavity. Based on the model proposed, the distortion effect on the vibro-acoustic behavior of the coupled system is investigated using the averaged sound pressure level inside the enclosure and the averaged quadratic velocity of the vibrating plate. Simulations are conducted to examine the distortion effect on acoustic natural frequencies, acoustic pressures and structural responses. Effects of the wall inclination on coupling coefficients are also assessed, and an index is proposed to quantify the degree of variation of coupling strength.

Keywords: Vibro-acoustic analysis; Coupling; Rectangular-like cavity; Tilted wall

1. Introduction

The noise radiated by a vibrating structure into an enclosed cavity is of particular interest for many industrial applications. Typical examples include cabin noise inside vehicles and aircraft fuselages, which are usually modeled by a cavity enclosed by a flexible

* Corresponding author. Tel: +852 2766 6769; fax: +852 2365 4703.
E-mail addresses: mmyylee@polyu.edu.hk (Y.Y. Li), mmlcheng@polyu.edu.hk (L. Cheng).
[1] Tel: +852 2766 6669; fax: +852 2365 4703.

0003-682X/$ - see front matter © 2006 Elsevier Ltd. All rights reserved.
doi:10.1016/j.apacoust.2006.04.005

vibrating structure. The coupled structural vibration and acoustic field form a so-called vibro-acoustic system. Vibro-acoustic analyses of these systems have been extensively carried out using various analytical and experimental methods in the past. Early researches in this field were presented by Junger and Feit [1] and Dowell *et al.* [2,3], who developed a comprehensive modal-based theoretical framework for interior sound field prediction. Since then, a large amount of efforts has been devoted to investigating the vibro-acoustic behavior of such systems, such as analysis of structural–acoustic modal interaction [4–7] and sound radiation prediction [8–11].

In general, structural vibration radiates sound into the enclosure through its coupling with acoustic modes. Therefore, an accurate characterization of the sound–structural interaction is essential for the prediction of acoustic field. Since conventional modal-based methods heavily rely on the availability of the acoustic modes, which are not analytically known in the presence of geometry irregularity, most of previous investigations focused on systems with perfect geometry and homogeneous structural properties [7–10]. In practice, imperfections (geometrical distortion or structural parameter uncertainty) always exist to a certain extent, which may lead to significant discrepancy from results obtained using idealized models, in terms of both eigen-frequencies and responses of the system. In most cases, this problem is not critical since the induced discrepancy is usually gentle and small so that numerical simulations using perfect system can still be applicable to some extent. However, there are circumstances under which the discrepancy becomes very subtle and large. One indication is that in some vibro-acoustic systems, numerical results cannot match the experimental ones [12].

Some techniques and methods have been developed so far to address the increasing interest in the distortion effect on sound–structure interactions [13,14]. Using the acousto-elastic theory, acoustic modal properties of irregular-shaped cavities were computed by approximating the cavity geometry with a set of rectangular subcavities [15]. Based on the Green theorem, Succi calculated the interior acoustic field in an automobile cabin, and the effects of arbitrary shape on the eigenvalues of the system were investigated [16]. In our previous work, a "combined integro-modal approach" was proposed to predict acoustic properties of irregular-shaped cavities [17]. The development of these techniques makes it possible to handle the cavities with irregular shapes in a semi-analytical way. All aforementioned works, however, mainly focused on the prediction of the natural frequencies of cavities and seldom addressed the coupling issue and the possible effects of the geometrical irregularity on system responses. A first attempt was made by extending the combined integro-modal approach to analyze the coupling characteristics between a vibrating panel and an irregular-shaped cavity with a tilted wall [18]. Using the coupling coefficients, effects on the coupling between acoustic modes and structural modes were examined, and it was found that the geometric distortion may dramatically change the coupling nature to thwart the prediction using perfect model. Again, no attention was paid to the effect of wall inclination on the vibro-acoustic behavior of the whole system.

This paper is a continuation of that work [18] and attempts to provide some answers to this problem. A model is first developed to handle the full vibro-acoustic coupling of a vibrating plate backed by an acoustically hard-walled enclosure with a tilted wall, which is introduced to represent the geometrical distortion. The averaged sound pressure level inside the enclosure and the averaged quadratic velocity of the panel are used, respectively, to examine the distortion effect on the acoustic field inside the enclosure and the vibration of

plate. Since the coupling is the key to control the energy conversion from vibrating plate to acoustic cavity, investigations on the distortion effect on modal couplings are then carried out. The relationship between the coupling coefficients with and without wall inclination is investigated. Numerical simulations are conducted leading to some useful conclusions.

2. Formulation

2.1. Vibro-acoustic modeling

The structure under investigation is a rectangular-like enclosure with one tilted wall (a trapezoidal enclosure) covered with a homogeneous and isotropic vibrating panel, as shown in Fig. 1. The enclosure has a volume V (cavity with solid lines) surrounded by a surface $S_{\text{ori}} = S_1 \cup S_2 \cup \cdots$. A slightly inclined surface S_1 characterized by an inclination angle α, is introduced to represent the geometrical distortion from the standard rectangular geometry. Apart from the surface S_2 occupied by the panel which is simply-supported, all other surrounding walls are assumed to be acoustically rigid.

The vibration of the panel under a plane wave excitation $\widetilde{P}(x,y,t)$ is governed by the following equation [3]

$$D\nabla^4 w + \rho h_t \frac{\partial^2 w}{\partial t^2} = \widetilde{P}(x,y,t) - P_c(z=h), \tag{1}$$

where w, D, ρ and h_t are the transverse displacement (positive downwards), the flexible rigidity, the density and the thickness of the panel, respectively. P_c is the acoustic pressure inside the cavity.

In general, the total pressure acting on the panel, $\widetilde{P}(x,y,t)$, can be decomposed into three parts, *i.e.* the incident pressure, the reflected pressure when the panel is assumed rigid and the radiated pressure due to the panel vibration. It is generally accepted that the

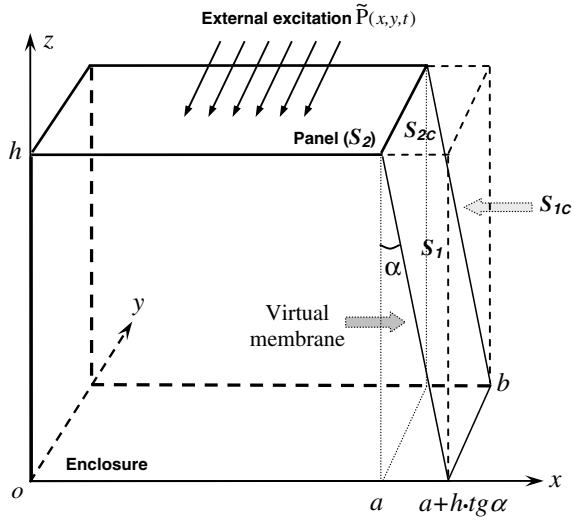

Fig. 1. Schematic diagram of a rectangular-like enclosure with a tilted wall covered with a vibrating panel.

radiated pressure is rather low compared to the other two components. Therefore, by neglecting the radiated pressure towards outside and assuming equal magnitudes for the incident and reflected pressure waves, the excitation pressure on the panel is twice the magnitude of the incident wave, known as blocked pressure [19]

$$\begin{aligned}\tilde{P}(x,y,t) &= 2P_o \exp(\vec{j}\omega t - \vec{j}k_o z\cos\phi - \vec{j}k_o x\sin\phi\cos\theta - \vec{j}k_o y\sin\phi\sin\theta)\\ &= \widetilde{P}_o(\phi,\theta)\mathrm{e}^{\vec{j}\omega t}\end{aligned} \tag{2}$$

in which P_o is the amplitude of the incident pressure, ϕ and θ are the elevation angle and azimuth angle, respectively. $k_o = \omega/c$ is the wave number with c being the sound speed.

Following the conventional modal superposition theory, w is decomposed over the mode shape functions $\varphi_{ij}(x,y)$ of the panel under the modal coordinate $q_{ij}(t)$, *i.e.*,

$$w(x,y,t) = \sum_{i=1}^{I}\sum_{j=1}^{J}\varphi_{ij}(x,y)q_{ij}(t), \quad \varphi_{ij}(x,y) = \sin\frac{\mathrm{i}\pi x}{a}\sin\frac{\mathrm{j}\pi y}{b}. \tag{3a, b}$$

Substituting Eqs. (3a,b) into (1) and taking into account the viscous damping terms ζ_{ij}, one has

$$\begin{aligned}&m_{ij}(\ddot{q}_{ij}(t) + 2\zeta_{ij}\omega_{ij}\dot{q}_{ij}(t) + \omega_{ij}^2 q_{ij}(t)) = \int_{S_2}(\widetilde{P}(x,y,t) - P_{\mathrm{c}}(z=h))\varphi_{ij}\,\mathrm{d}s,\\ &\quad i = 1,\ldots,I;\ j = 1,\ldots,J.\end{aligned} \tag{4}$$

where ω_{ij} and m_{ij} are the ijth natural angular frequency and the generalized mass of the ijth mode of the panel, respectively.

The acoustic pressure P_{c} inside the enclosure satisfies the wave equation

$$\nabla^2 P_{\mathrm{c}} - \frac{1}{c^2}\frac{\partial^2 P_{\mathrm{c}}}{\partial t^2} = 0 \tag{5}$$

with boundary conditions

$$\frac{\partial P_{\mathrm{c}}}{\partial \mathbf{n}} = \begin{cases}\rho_{\mathrm{c}}\ddot{w} & \text{on the panel,}\\ 0 & \text{on the rigid wall,}\end{cases} \tag{6}$$

where ρ_{c} is the equilibrium fluid density and $\mathbf{n}$ the normal direction towards outside.

For the trapezoidal enclosure V, P_{c} cannot be decomposed on the basis of acoustic modes, which are difficult to be known analytically. We therefore used the "combined integro-modal approach" to handle the acoustic pressure inside the enclosure V [17]. In the present case, a rectangular bounding cavity enclosing V and occupying a volume V_{c} $((a + h\cdot tg\alpha)bh)$ with a surface S_{c} ($S_{\mathrm{c}} = S_{1\mathrm{c}} \cup (S_{2\mathrm{c}} + S_2) \cup \cdots$) is constructed. The natural modes of the bounding cavity are adopted for sound pressure decomposition. Therefore, P_{c} is decomposed on modal basis ψ_{lmn} of the bounding cavity V_{c} as

$$P_{\mathrm{c}} = \sum_{l=0}^{L}\sum_{m=0}^{M}\sum_{n=0}^{N}\psi_{lmn}P_{\mathrm{c},lmn}(t), \quad \psi_{lmn} = \cos\left(\frac{l\pi x}{a + h\cdot tg\alpha}\right)\cos\left(\frac{m\pi y}{b}\right)\cos\left(\frac{n\pi z}{h}\right), \tag{7a, b}$$

where (L, M, N) are the numbers of the terms to be kept after the truncation of the series.

Using the Green's theorem [3] and introducing a modal loss factor ζ_{lmn}, Eq. (5) can be transformed into a set of acoustic equations as

$$\sum_{r=0}^{L}\sum_{s=0}^{M}\sum_{t=0}^{N}\left[m_{lmn,rst}(\ddot{P}_{c,rst}(t)+2\zeta_{lmn}\omega_{lmn}\dot{P}_{c,rst}(t)+\omega_{lmn}^2P_{c,rst}(t))+\frac{c^2}{V}n_{lmn,rst}P_{c,rst}(t)\right]$$
$$=\frac{\rho_c S_2c^2}{V}\sum_{i=1}^{I}\sum_{j=1}^{J}L_{lmn,ij}\ddot{q}_{ij}(t),\quad l=0,\ldots,L;\ m=0,\ldots,M;\ n=0,\ldots,N. \tag{8}$$

where

$$m_{lmn,rst}=\frac{1}{V}\int_V\psi_{lmn}\psi_{rst}\,d\upsilon,\quad \omega_{lmn}^2=c^2\left\{\left(\frac{l\pi}{a+h\cdot tg\alpha}\right)^2+\left(\frac{m\pi}{b}\right)^2+\left(\frac{n\pi}{h}\right)^2\right\},$$
$$n_{lmn,rst}=\int_{S_1}\psi_{rst}\frac{\partial\psi_{lmn}}{\partial\mathbf{n}}\,ds\quad\text{(refer to [18] for detail)}, \tag{9}$$
$$L_{lmn,ij}=\frac{1}{S_2}\int_{S_2}\psi_{lmn}\varphi_{ij}\,ds.$$

In the case of harmonic excitation, $q_{ij}(t)=B_{ij}e^{\vec{j}\omega t}$ and $P_{c,rst}(t)=C_{rst}e^{\vec{j}\omega t}$, Eqs. (4) and (8) can be rewritten as

$$m_{ij}(-\omega^2+2\vec{j}\zeta_{ij}\omega_{ij}\omega+\omega_{ij}^2)B_{ij}+S_2\sum_{l=0}^{L}\sum_{m=0}^{M}\sum_{n=0}^{N}L_{lmn,ij}C_{lmn}=\int_{S_2}\widetilde{P}_o(\phi,\theta)\varphi_{ij}\,ds,$$
$$i=1,\ldots,I;\ J=1,\ldots,J. \tag{10}$$
$$\sum_{r=0}^{L}\sum_{s=0}^{M}\sum_{t=0}^{N}\left[m_{lmn,rst}(-\omega^2+2\vec{j}\zeta_{lmn}\omega_{lmn}\omega+\omega_{lmn}^2)+\frac{c^2}{V}n_{lmn,rst}\right]C_{rst}$$
$$=-\frac{\rho_c S_2c^2\omega^2}{V}\sum_{i=1}^{I}\sum_{j=1}^{J}L_{lmn,ij}B_{ij},\quad l=0,\ldots,L;\ m=0,\ldots,M;\ n=0,\ldots,N. \tag{11}$$

Rearranging Eqs. (10) and (11) in the matrix form gives

$$\begin{bmatrix}\mathbf{H}_{11} & S_2\mathbf{L}\\ \kappa S_2\mathbf{L}^{\mathrm{T}} & \mathbf{H}_{22}\end{bmatrix}\begin{Bmatrix}B_{11}\\ \cdots\\ B_{IJ}\\ C_{000}\\ \cdots\\ C_{LMN}\end{Bmatrix}=\begin{Bmatrix}\int_{S_2}\widetilde{P}_o\varphi_{11}\,ds\\ \cdots\\ \int_{S_2}\widetilde{P}_o\varphi_{IJ}\,ds\\ 0\\ \cdots\\ 0\end{Bmatrix}, \tag{12}$$

where $\mathbf{H}_{11}$, $\mathbf{L}$ and H_{22} are matrices related to the structural dynamics, the structure–acoustic coupling and the enclosure acoustic behavior, respectively,

$$\mathbf{H}_{11}=\begin{bmatrix}\ddots & & \\ & m_{ij}(\omega_{ij}^2+2\vec{j}\zeta_{ij}\omega_{ij}\omega-\omega^2) & \\ & & \ddots\end{bmatrix},\quad \mathbf{L}=\begin{bmatrix}L_{000,11} & \cdots & L_{LMN,11}\\ \cdots & \cdots & \cdots\\ L_{000,IJ} & \cdots & L_{LMN,IJ}\end{bmatrix},\quad \kappa=\frac{\rho_c c^2\omega^2}{V},$$
$$\mathbf{H}_{22}=\frac{c^2}{V}\begin{bmatrix}\cdots & \cdots & \cdots\\ \cdots & n_{lmn,rst} & \cdots\\ \cdots & \cdots & \cdots\end{bmatrix}+\begin{bmatrix}\ddots & & \\ & (\omega_{lmn}^2+2\vec{j}\zeta_{lmn}\omega_{lmn}\omega-\omega^2) & \\ & & \ddots\end{bmatrix}\cdot\begin{bmatrix}\cdots & \cdots & \cdots\\ \cdots & m_{lmn,rst} & \cdots\\ \cdots & \cdots & \cdots\end{bmatrix}. \tag{13}$$

Eq. (12) describes the vibro-acoustic behavior of the system, taking into account the effect of wall inclination and the full coupling between the panel and the enclosure. It is used to calculate various coefficients for constructing the acoustic pressure inside the enclosure and the vibration of the panel, which are usually examined by the averaged sound pressure level

$$L_{\mathrm{P}} = 10\log(\langle P_{\mathrm{c}}^2\rangle / P_{\mathrm{ref}}^2), \tag{14a}$$

and the averaged quadratic velocity

$$L_{\mathrm{w}} = \frac{\omega^2}{2S_2}\int_{S_2} ww^* \,\mathrm{d}s, \tag{14b}$$

where $\langle P_{\mathrm{c}}^2\rangle = \frac{1}{2V}\int_V P_{\mathrm{c}}P_{\mathrm{c}}^* \,\mathrm{d}v$, $p_{\mathrm{ref}} = 20\ \mu\mathrm{Pa}$. L_{w} is expressed in dB referenced to $2.5\times10^{-15}\ \mathrm{m^2/s^2}$ and the asterisk denotes complex conjugate.

2.2. Coupling analysis

In light of Eq. (12), the structure–acoustic coupling plays an important role in determining the vibro-acoustic behavior of the whole system. It is clear that, in order to avoid excessive noise and vibration transfer into the enclosure, relevant structural and acoustic modes need to be decoupled from each other. Therefore, a suitable quantification of the distortion effect on structure–acoustic coupling is very useful to gain a basic understanding on the sound–structure interaction and noise generation.

In general, the coupling between the *lmn*th acoustic mode $\tilde{\psi}_{lmn}(\alpha)$ of the cavity with a tilted wall and the *ij*th structural mode φ_{ij} can be expressed by the coupling coefficient $\tilde{L}_{lmn,ij}(\alpha)$ defined as

$$\widetilde{L}_{lmn,ij}(\alpha) = \frac{1}{S_2}\int_{S_2} \tilde{\psi}_{lmn}(\alpha)\cdot\varphi_{ij}\,\mathrm{d}s. \tag{15}$$

It should be mentioned that in the following discussions, the terms "acoustic mode (l,m,n)" and "structural mode (i,j)" will be used to represent the modes of the coupled system dominated by the enclosure and the panel, respectively. Although the notation has clear physical meaning for acoustic modes when $\alpha = 0$, it is loosely used for the cavity with a tilted wall for the sake of convenience. In the latter case, it simply stands for a mode evolving from the *lmn*th acoustic mode ($\alpha = 0$) due to the wall inclination.

Considering that $\tilde{\psi}_{lmn}(\alpha)$ cannot be analytically known for the irregular-shaped cavity, an approximate expression using the combination of basic modes ($\alpha = 0$) is hence adopted,

$$\tilde{\psi}_{lmn}(\alpha) = \sum_{r,s,t} C_{lmn,rst}\psi_{rst}. \tag{16}$$

Substituting (16) and (3b) into Eq. (15) yields

$$\widetilde{L}_{lmn,ij}(\alpha) = \sum_{r,s,t} C_{lmn,rst}(-1)^{\mathrm{t}}\frac{ij[(-1)^{s+j}-1]\cdot\gamma_{ir}(\alpha)}{\pi^2(s^2-j^2)}, \quad s\neq j, \tag{17}$$

where

$$\gamma_{ir}(\alpha) = \left((-1)^i\cos\frac{r\pi}{1+(h/a)tg\alpha} - 1\right) \Bigg/ \left(\left(\frac{r}{1+(h/a)tg\alpha}\right)^2 - i^2\right). \tag{18}$$

In the case $\alpha = 0$, $\tilde{\psi}_{lmn}(\alpha) = \psi_{lmn}$ and $\widetilde{L}_{lmn,ij}(\alpha = 0) = L_{lmn,ij}$ defined in Eq. (9), *i.e.*, one has [20],

$$\widetilde{L}_{lmn,ij}(\alpha = 0) = L_{lmn,ij} = \begin{cases} (-1)^n \frac{ij[(-1)^{m+j}-1][(-1)^{l+i}-1)}{\pi^2(l^2-i^2)(m^2-j^2)}, & l \neq i, (l+i)/2 \neq \text{integer} \\ & m \neq j, (m+j)/2 \neq \text{integer} \\ 0 \quad \text{otherwise} \end{cases} \tag{19}$$

In the general case, it can be shown that

$$\widetilde{L}_{lmn,ij}(\alpha) = \sum_{\substack{r,s,t \\ \frac{(i+r)}{2} \neq \text{integer}}} C_{lmn,rst} L_{rst,ij} \frac{(i^2 - r^2)\gamma_{ir}(\alpha)}{2} + \sum_{\substack{r,s,t \\ \frac{(i+r)}{2} = \text{integer}}} C_{lmn,rst}(-1)^t \frac{ij[(-1)^{s+j} - 1]\gamma_{ir}(\alpha)}{\pi^2(s^2 - j^2)}, \quad s \neq j. \tag{20}$$

Eq. (20) describes the variation of coupling coefficients under the geometrical distortion α. Different from $L_{rst,ij}$ which only depends on the orders of modes (Eq. (19)), $\widetilde{L}_{lmn,ij}(\alpha)$ comprises a combination of $L_{rst,ij}$, which includes the contribution of additionally evoked modes due to the distortion, as reflected by the second part of Eq. (20). Obviously, the existence of distortion also alters the coupling coefficients through introducing the variable $\gamma_{ir}(\alpha)$, and therefore resulting in an alteration of vibro-acoustic behavior of the system.

3. Results and discussions

Numerical analyses are conducted using the configuration shown in Fig. 1 with a dimension of $a \times b \times h = 0.92 \times 0.15 \times 0.6\ \text{m}^3$. The thickness of the aluminum panel is set as $h_t = 0.002$ m, and the modal loss factor is assigned to be 0.005 for the panel while 0.001 for the cavity. α is varied from 0° to 10° to simulate the geometrical distortion.

The number of modes used for structural displacement and sound pressure decomposition is the main factor affecting the accuracy of the solution. In general, the accuracy can be satisfied by increasing the number of modes until convergence is achieved in the frequency range of interest. In the present case, a careful convergence study was carried out by increasing the number for each variable involved in the modal expansion series, leading to the following selection: $(60, 3, 10)$ for the enclosure and $(10, 10)$ for the panel.

The validation of the model was verified by examining a system with a slight inclination angle $\alpha = 0.001°$. Comparison between the averaged sound pressure level for this configuration with that for a perfect one ($\alpha = 0$, verified in [21] using an enclosure covered with a single panel) shows a good agreement (not shown here).

3.1. Distortion effect on vibro-acoustic responses of the coupled system

Fig. 2(a) shows the averaged sound pressure levels L_p inside the enclosure when $\alpha = 0°$, 5° and 10° under an oblique plane wave excitation. Peaks marked with symbols '■' and '▲' stand for resonances dominated by the enclosure and the panel, respectively. Apparent effects of the wall inclination on L_p can be noticed especially with a larger α value. These effects are reflected by an alteration in the level of responses in several frequency regions,

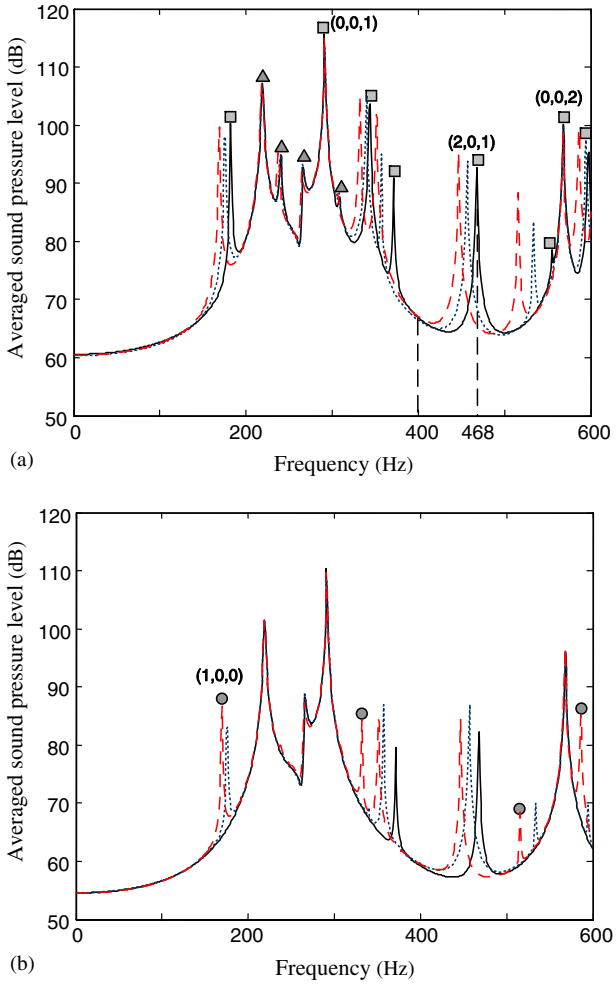

Fig. 2. Averaged sound pressure level L_p (a) an oblique plane wave with $\phi = 60°$ and $\theta = 30°$; and (b) a normal plane wave. Both are with amplitude of 1 Pa. $\alpha = 0$: ——; $\alpha = 5°$: ····· ; $\alpha = 10°$: – – –. ■, ●: modes dominated by the enclosure; ▲: modes dominated by the panel.

especially in those dominated by the acoustic resonances. Focusing on those cavity modes, it can be seen that within the analyzed frequency range [0 600]Hz, the left-shift of peaks occurs except for modes $(0,0,1)$ and $(0,0,2)$, and the variation is getting larger when α increases. The reason is that an increased α alters the dimension of the cavity in x-direction, leading to an increase of wavelengths λ_{lmn} and a corresponding decrease of acoustic natural frequencies $f_{lmn}(l \neq 0,\ c/f_{lmn} = \lambda_{lmn})$ [18]. However, the effect of the wall inclination on the structural modes is trivial.

A further confirmation comes from Fig. 2(b), in which a normal plane wave excitation is applied to the panel. In addition, compared with the case when $\alpha = 0$, the wall inclination provokes the excitation of additional acoustic modes (denoted by "●") due to the destruction of the symmetry of enclosure geometry. In such circumstance, the effects of the distortion become significant.

The effect of distortion on the distribution of the acoustic pressure at different frequencies is then examined. Two particular frequencies are chosen for this purpose, one is the resonance frequency ($f(\alpha = 0) = 468$ Hz), and the other is a frequency ($f(\alpha = 0) = 400$ Hz) at which the wall inclination has no apparent effect on the overall sound pressure level. The acoustic pressure distributions along the cross-section $y = b/4$ at the frequency 468 Hz for $\alpha = 0°$ and 10° are shown in Fig. 3(a) and (b), respectively. Since $f(\alpha = 0) = 468$ Hz corresponds to the resonant frequency of the mode $(2, 0, 1)$ (as clearly shown by Fig. 2(a)), the acoustic pressure distribution of this mode is significantly modified with the introduction of the inclination angle $\alpha = 10°$, *e.g.*, the maximal pressure amplitude reduces to 0.3% (Fig. 3(b)) of its counterpart at $\alpha = 0$, which is quite understandable. Another frequency of interest is $f = 400$ Hz, at which the L_p curves for different α are overlapped. Fig. 3(c) and (d) illustrate the pressure distribution for $\alpha = 0°$ and 10°, respectively. It can be observed that, even though no significant changes are observed from the overall sound pressure level, the acoustic pattern, especially in the vicinity of the tilted wall, is altered to some extent due to the inclination of the wall.

As far as the vibration of the panel is concerned, Fig. 4 illustrates the averaged quadratic velocity L_w for $\alpha = 0°$, 5° and 10°. Generally speaking, structural modes, especially the low frequency mode $(1, 1)$, dominate the vibration response of the panel. The acoustic mode $(0, 0, 1)$ is also well evoked due to the closeness between the natural frequency of this mode ($f_{001} = 291$ Hz) and that of the structural mode $(4, 1)$ ($f_{41} = 308$ Hz). However, those acoustic modes which are affected by the wall inclination create weak impact on the structural

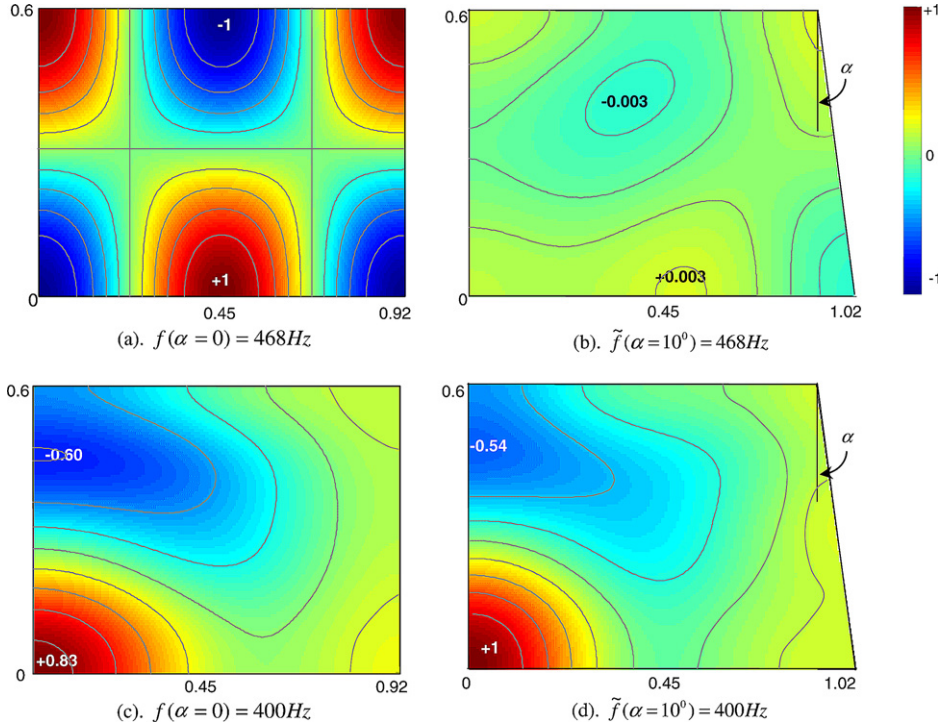

Fig. 3. Acoustic pressure distribution at the cross-section $y = b/4$ of the enclosure.

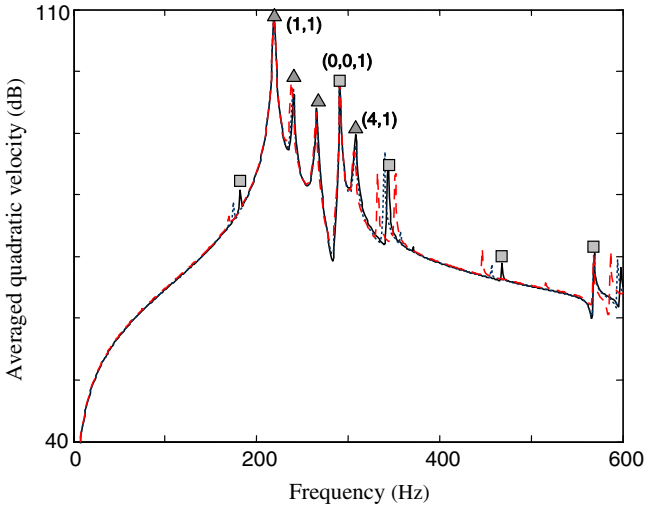

Fig. 4. Averaged quadratic velocity L_w of the panel for $\alpha = 0$, 5° and 10°. $\alpha = 0$: ——; $\alpha = 5°$: ·····; $\alpha = 10°$: – – –. ■: modes dominated by the enclosure; ▲: modes dominated by the panel.

responses. Obviously, the vibration of panel is not so sensitive to distortion compared with the acoustic field inside the enclosure.

3.2. Distortion effect on modal coupling

Theoretically speaking, if a particular acoustic mode is not coupled with any structural mode, no energy will be converted into the cavity from that mode. Obviously, it is not possible to find such a α so that the coupling coefficients $\widetilde{L}_{lmn,ij}(\alpha) = 0$ ($i = 1,\ldots,I$; $j = 1,\ldots,J$). As mentioned in Section 2.2, the effect of α on structure–acoustic coupling can be assessed by investigating the variation of $\widetilde{L}_{lmn,ij}(\alpha)$. Fig. 5(a) and (b) illustrate the histogram of $\widetilde{L}_{lmn,ij}(\alpha)$ for $\alpha = 0°$ and 10°, respectively. It can be seen that for $\alpha = 0°$, due to the orthogonality of the modal functions of the cavity, any symmetric structural mode is decoupled with an acoustic mode which is anti-symmetrical in one of the two directions parallel to the panel edges, leading to a relatively simple and selective coupling pattern. When $\alpha = 10°$, however, the very selective property of the coupling for $\alpha = 0$ is no longer valid. Instead, more modes are evoked resulting in a complicated coupling behavior. This can be clearly seen by comparing Fig. 5(a) with (b). For example, among the analyzed structural modes $((1,1),\ldots,(2,4))$, *two* more, *i.e.*, (2,1) and (2,3), are coupled to the acoustic mode (2,0,0) for $\alpha = 10°$ compared with the case of $\alpha = 0$, in which only (1,1) and (1,3) are involved. In addition, observing the amplitude of $\widetilde{L}_{lmn,ij}(\alpha)$ shows that, although the maximal $L_{lmn,ij}(\alpha)$ keeps almost unchanged, the effect of the evoked structural modes on the coupling is significant for some acoustic modes, *e.g.*, for mode (2,1,2), the variation of $\widetilde{L}_{212,22}(\alpha = 10°)$ reaches 29% of the maximal one. This observation implies that a slight geometrical imperfection of the cavity can drastically change the coupling nature to thwart the prediction using perfect model. This is a plausible reason to explain the inconsistency between numerical results and experimental ones for some vibro-acoustic systems, in which the existence of slight geometrical

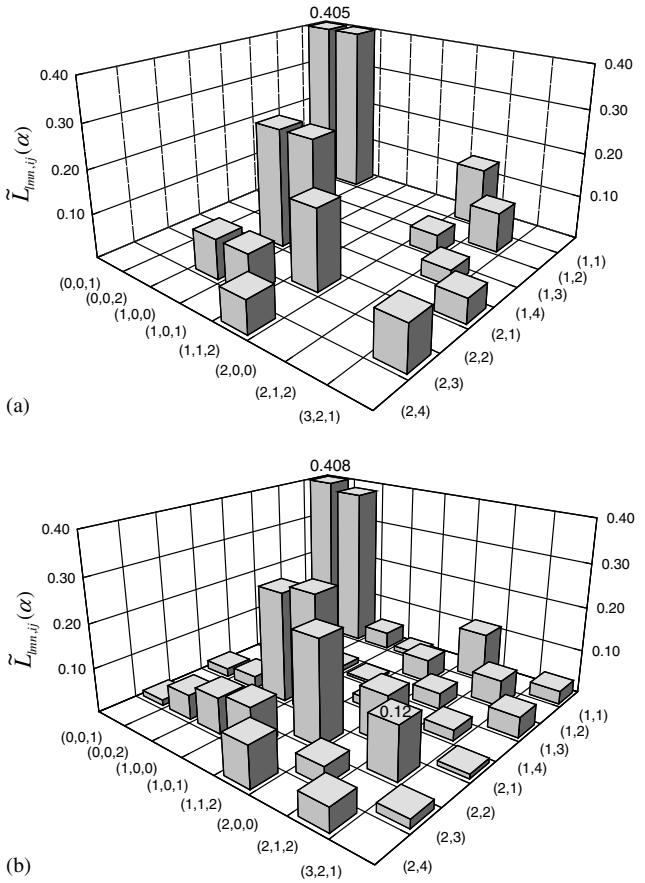

Fig. 5. Histogram of coupling coefficients $\widetilde{L}_{lmn,ij}(\alpha)$ (in absolute value) for (a) $\alpha = 0$ and (b) $\alpha = 10°$.

imperfection in experiments introduces uncertainties into the system through changing structure–acoustic coupling strength.

A quantitative analysis on the effect of α on one particular acoustic mode is carried out by defining the degree of variation in coupling strength as follows:

$$\chi_{lmn}(\alpha) = \sqrt{\frac{1}{IJ}\cdot\sum_{i,j}\left(\left(\widetilde{L}_{lmn,ij}(\alpha) - \widetilde{L}_{lmn,ij}(\alpha=0)\right)/\max_{i,j}\left(\widetilde{L}_{lmn,ij}(\alpha=0)\right)\right)^2},$$
$$i = 1,\ldots,I;\ j = 1,\ldots,J. \tag{21}$$

In a sense, the above definition reflects the degree of changes in the coupling coefficients relative to the ideal case when $\alpha = 0$. Fig. 6 illustrates the tendency plot of $\chi_{lmn}(\alpha)$ with α varying from 0° to 10°. It can be seen that $\chi_{lmn}(\alpha)$ increases remarkably with the increase of distortion, showing a strong effect of evoked structural modes on the coupling. For example, with $\alpha = 10°$, the two evoked structural modes $(2,1)$ and $(2,3)$, lead to more than 20% variation in $\chi_{lmn}(\alpha)$ for the acoustic mode $(2,0,0)$. Another observation is that the coupling nature is altered with the increase of α. As an example, when $\alpha = 2°$, the mode $(2,0,1)$ dominates $\chi_{lmn}(\alpha)$, followed by $(2,0,0)$, $(1,0,0)$, $(1,0,2)$ and $(0,0,2)$. The situation

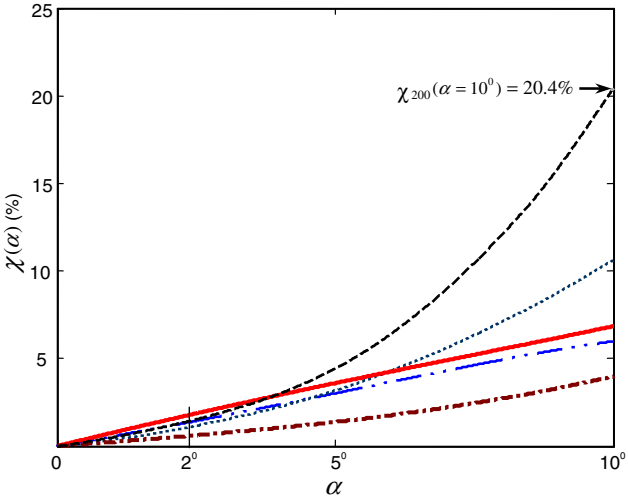

Fig. 6. Degree of variation of coupling strength $\chi_{lmn}(\alpha)$ with α varying from 0° to 10°: —··–: (1,0,0); –·–: (0,0,2); ·····: (1,0,2); – – –: (2,0,0); ——: (2,0,1).

is different when α increases. The effect of mode (2,0,1) on $\chi_{lmn}(\alpha)$ is significantly weakened. Instead, the mode (2,0,0) becomes the most dominant, followed by the modes (1,0,2), and leads to a vary large extent when $\alpha = 10°$. One should expect this change in coupling strength to subsequently alter the noise generation.

4. Conclusions

This paper presents a vibro-acoustic modeling and analysis of a rectangular-like cavity with a tilted wall coupled to a vibrating plate. Different from previous studies, emphasis is put on analyzing the distortion effect on the vibro-acoustic behavior and the coupling mechanism of the system, leading to the following conclusions.

(1) Characterized by the averaged sound pressure level L_p, changes in the acoustic natural frequencies and acoustic pressure distribution inside the cavity are clearly identified even for a small distortion. Given the normal plane wave excitation, more effective structural–acoustic coupling takes place due to geometrical distortion. However, the distortion effect on the vibration of panel is trivial, suggesting that the feedback effect of slight distortion of the cavity can be neglected during vibration analysis of the panel so as to simplify the calculation.
(2) A slight distortion of the enclosure can lead to a noticeable alteration in the structure–acoustic coupling, and subsequently the acoustic field inside the enclosure. This is probably the reason why some predictions using idealized models fail to match experimental results.

Acknowledgements

The authors thank the Research Committee of The Hong Kong Polytechnic University for the financial support to this project (G-U031). Li Cheng acknowledges the support

from a special fund for recently promoted Chair Professors given by The Hong Kong Polytechnic University.

References

[1] Junger M, Feit D. Sound, structures and their interaction. MIT Press; 1972.
[2] Dowell EH, Voss HM. The effect of a cavity on panel vibration. AIAA J 1963;1:476–7.
[3] Dowell EH, Gorman GF, Smith DA. Acoustoelasticity: general theory, acoustic natural modes and forced response to sinusoidal excitation, including comparisons with experiment. J Sound Vib 1977;52:519–41.
[4] Peretti LF, Dowell EH. Asymptotic modal-analysis of a rectangular acoustic cavity excited by wall vibration. AIAA J 1992;30:1191–8.
[5] Wyckaert K, Augusztinovicz F, Sas P. Vibro-acoustical modal analysis: reciprocity, model symmetry, and model validity. J Acoust Soc Am 1996;100:3172–81.
[6] Franzoni LP, Bliss DB. A discussion of modal uncoupling and an approximate closed-form solution for wealy-coupled systems with application to acoustics. J Acoust Soc Am 1998;103:1923–32.
[7] Sum KS, Pan J. On acoustic and structural modal cross-couplings in plate-cavity systems. J Acoust Soc Am 2000;107:2021–38.
[8] Keltie RF, Peng H. The effects of modal coupling on the acoustic power radiation from panels. J Vib Acoust Stress Rel Des 1987;109:48–54.
[9] Pan J, Bies DA. The effect of fluid–structural coupling on sound waves in an enclosure – theoretical part. J Acoust Soc Am 1990;87:691–707.
[10] Cunefare KA. Effect of modal interaction on sound radiation from vibrating structures. AIAA J 1992;30:2819–28.
[11] Kronast M, Hildebrandt M. Vibro-acoustic modal analysis of automobile body cavity noise. Sound Vib 2000;34:20–3.
[12] Rebillard E, Laulagnet B, Guyader JL. Influence of an embarked spring-mass system and defects on the acoustical radiation of a cylindrical shell. Appl Acoust 1992;36:87–106.
[13] Petyt M, Lea J, Koopman GH. A finite element method for determining the acoustic modes of irregular shaped cavities. J Sound Vib 1976;45:497–502.
[14] Brebbia CA, Telles JCF, Wrobel LC. Boundary element techniques. New York: Springer; 1984.
[15] Chao CF, Dowell EH, Bliss DB. Modal analysis of interior noise field. In: Proceedings of the vibration conference of the design engineering technical conferences. New York: ASME; 1981. p. 30–56.
[16] Succi GP. The interior acoustic field of an automobile cabin. J Acoust Soc Am 1987;81:1688–94.
[17] Missaoui J, Cheng L. A combined integro-modal approach for predicting acoustic properties of irregular-shaped cavities. J Acoust Soc Am 1997;101:3313–21.
[18] Li YY, Cheng L. Modifications of acoustic modes and coupling due to a leaning wall in a rectangular cavity. J Acoust Soc Am 2004;116:3312–8.
[19] Carneal JP, Fuller CR. An analytical and experimental investigation of active structural acoustic control of noise transmission through double panel systems. J Sound Vib 2004;272:749–71.
[20] Snyder SD, Hansen CH. The design of systems to control actively periodic sound transmission into enclosed space, part 2: mechanisms and trends. J Sound Vib 1994;170:451–72.
[21] Cheng L, Li YY, Gao JX. Energy transmission in a mechanically-linked double-wall structure coupled to an acoustic enclosure. J Acoust Soc Am 2005;117:2742–51.